

Surveying Hidden Planets in Kepler Exoplanetary Systems Using Transit  
Timing Variations

Abigail Graham

A senior thesis submitted to the faculty of  
Brigham Young University  
in partial fulfillment of the requirements for the degree of  
Bachelor of Science

Darin Ragozzine, Advisor

Department of Physics and Astronomy  
Brigham Young University

Copyright © 2021 Abigail Graham

All Rights Reserved



## ABSTRACT

### Surveying Hidden Planets in Kepler Exoplanetary Systems Using Transit Timing Variations

Abigail Graham

Department of Physics and Astronomy, BYU  
Bachelor of Science

During its prime mission, the Kepler Space Telescope found over 700 systems with more than one transiting planet. These multiple planet systems (multis) are the most information rich and dynamically interesting of all exoplanets. We picked 46 multis where one planet was experiencing transit timing variations (TTVs) not obviously caused by the other known planets. TTVs are caused by interactions between planets and therefore can provide evidence of additional, hidden planets in these systems. We first tried to determine if the TTVs could be reasonably explained by the known planets. We then projected six possible hidden planets for each system and performed the same analysis on the hidden planet in the strongest resonance with the TTV-experiencing planet that was estimated to be stable. Five of our systems have good fits with the known planets, 39 have good fits with the hidden planet added, and two require more work to find a satisfactory answer. This work significantly improves our understanding of the architectures of some of the most interesting multis from Kepler.

Keywords: Kepler Space Telescope, exoplanets, transit timing variations, PhoDyMM



## ACKNOWLEDGMENTS

I would like to thank Dr. Ragozzine for all his support on this project. He has been an incredible mentor throughout my time at BYU. He has helped to encourage me and provided an environment in which I could thrive while learning about this universe. This project would not have been possible without his care and guidance.

I would also like to thank the BYU Department of Physics and Astronomy, College of Physical and Mathematical Sciences, and Dr. Ragozzine's NASA Grant for funding my research over the past three years. Their support has been instrumental in the course of this work.

Dr. Fabrycky at the University of Chicago has been a great help on this project. He has provided additional insight into several of the systems in this work and helped us to find solutions and refine our results.

I would like to thank the BYU Fall 2020 PHSCS 227 class for all of their help. The first part of this thesis was done in collaboration with the entire class. Without their support, this work would have been much longer in the making. Several class members continued their support after the semester, helping to refine system data and provide technical support for our analyses.

I would like to thank all the collaborators responsible for building the PhoDyMM tool. This program was of great use throughout this project.

And finally, I would like to thank my family and friends for all of their support and encouragement. In particular, my father has done so much to encourage my curiosity and desire to pursue further knowledge and understanding of the universe.



# Contents

<b>Table of Contents</b>	<b>vii</b>
<b>1 Introduction</b>	<b>1</b>
1.1 The Search for Exoplanets . . . . .	1
1.2 Kepler Multi-Systems . . . . .	4
1.3 Transit Timing Variations . . . . .	4
<b>2 Methods</b>	<b>7</b>
2.1 Known Planet Models . . . . .	8
2.2 Hidden Planet Models . . . . .	10
<b>3 Results and Discussion</b>	<b>15</b>
3.1 Results . . . . .	15
3.1.1 Systems with Best Fit Using Known Planets . . . . .	16
3.1.2 Systems with Best Fit Using Hidden Planet . . . . .	19
3.1.3 Systems with More Complicated Answers . . . . .	26
3.2 Conclusion . . . . .	26
<b>Appendix A System Descriptions</b>	<b>27</b>
A.1 System Description for Known Planet Models . . . . .	27
A.2 System Description for Hidden Planet Models . . . . .	28
A.3 System Descriptions for Complicated Systems . . . . .	35
<b>Appendix B Selected Best Fit Model Figures</b>	<b>37</b>
B.1 Best Fit for Known Models . . . . .	37
B.2 Best Fit for Hidden Models . . . . .	38
B.3 Best Fit for Complicated Systems . . . . .	38
<b>Appendix List of Figures</b>	<b>38</b>
<b>Bibliography</b>	<b>45</b>
<b>Index</b>	<b>49</b>





# Chapter 1

## Introduction

### 1.1 The Search for Exoplanets

The desire to find planets outside our solar system, known as exoplanets, has existed for hundred of years. Both science and science fiction have proposed wide and wild ideas about what such a possibility could mean. However, the difficulties inherent in the search for exoplanets meant it was only in 1992 that Aleksander Wolszczan and Dale Frail found the first definitive pair [1]. Since then, advancements in technology have allowed for a sharp increase in the number of confirmed exoplanets. Figure 1.1 shows the number of exoplanets found each year since the first detected in 1988, though this planet was not confirmed until 2002 [2, 3], grouped by the method of discovery.

The transiting method has been the most successful way of finding exoplanets. The transiting method tracks the brightness of a star and measures the periodic dimming caused by planets passing in front of it. This method is biased to large planets that are close to their stars and thus have short orbital periods [5]. A familiar example of the idea behind transits are solar eclipses. When the moon passes in front of the sun, there is a very obvious decrease in light for select areas on Earth. We can also measure when Venus passes in front of the Sun from our perspective through the use of

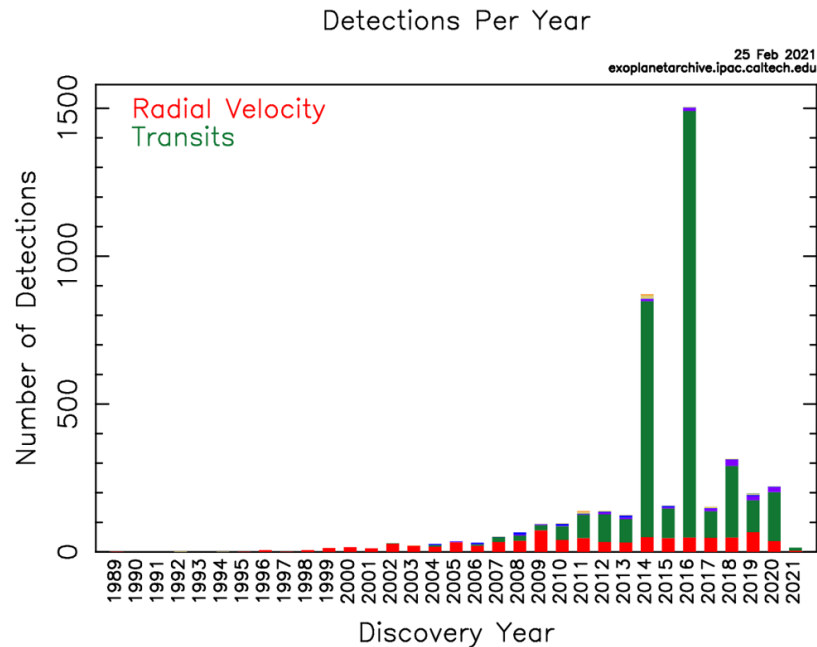


**Figure 1.1** Number of exoplanets discovered by year and discovery method. The peaks in 2014 and 2016 mark the main *Kepler Space Telescope* missions which were highly successful in finding exoplanets through transits [4].

telescopes.

The transit method can easily miss planets if they are slightly ( $\sim 2^\circ$ ) misaligned. Usually planets exterior to the known planets are missed since their larger distance from the star requires a smaller misalignment to be missed. However, it is possible and relatively common for intermediate or even interior planets to be missed due to the random observing direction [6].

The *Kepler Space Telescope* was created to be able to detect this periodic dimming in stellar brightness for stars other than our Sun. Launched in 2009, *Kepler* surveyed over 192,000 stars and found over 3,500 transiting exoplanets [7]. The largest bars seen in Figure 1.1 are from the *Kepler* mission. These detections, shown in Figure 1.2, cover a wide range of orbital periods and planetary sizes. Figure 1.2 also shows where some of the holes in *Kepler's* sensitivity are. For example, there is only one Earth-like exoplanet represented.

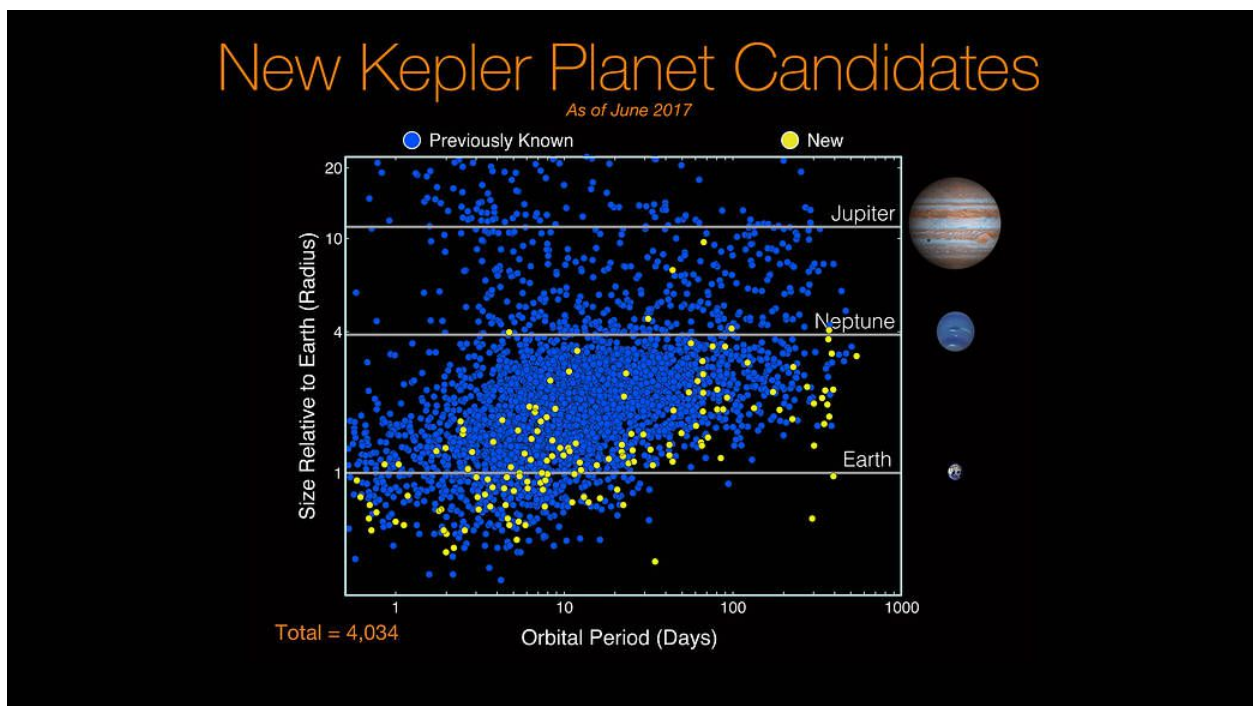


**Figure 1.2** New *Kepler* planet candidates as of June 2017 [8]. It can be seen that Kepler has found many exoplanets but it has some blind spots in what kind of planets it can easily detect. For example, there is only one Earth-like planet that has been detected.

## 1.2 Kepler Multi-Systems

As our solar system consists of 8 planets orbiting a single star, it is not too far to think it is likely other stars have multiple planets around them as well, called "multi-systems" or just "multis". *Kepler* found many such systems that are some of the most information-rich and dynamically-interesting systems to study [6]. For example, Kepler-90 is the first, and so far only, system found to match our solar system for number of planets [9].

To identify any potential planets found by *Kepler*, each object is given a Kepler Object of Interest (KOI) number. These identification numbers are based on the order the objects are found. For example "KOI-1601.01" would indicate the first object discovered in the system KOI-1601. There is some redundancy in identification methods and most systems are referred to by multiple names. For the purposes of this paper, we will use the KOI number in text. The tables featured later will include both KOI and the Kepler Input Catalog (KIC) numbers.

## 1.3 Transit Timing Variations

A benefit of studying multis is the opportunity to see how planets interact. Transit timing variations (TTVs) occur when a planet transits early or late creating a nonlinear ephemeris. An ephemeris shows what would be considered the proper time a given planet should transit its star. A nonlinear ephemeris occurs when a planet, for some reason, does not transit with exact periodicity (transiting either early or late as with TTVs) or does not transit for the same amount of time as with transit duration variations. TTVs are caused by gravitational interactions between planets and are typically on the scale of minutes. These variations are periodic themselves, the planet arriving early or late in a pattern set by the orbital and physical properties of the dynamically interacting planets. Two planets perturbing each other typically have TTV signals with opposite phases causing one to peak, or be the most early, while the other is at its latest [10]. Many of the multis found by *Kepler* show

TTVs between planets. When there is not an obvious reason for the observed TTVs in a planet, we call them unascrivable TTVs (uTTVs). These uTTVs can give us insight into the dynamics of the system that we can't observe directly, including providing evidence of additional bodies in the system. This technique has been applied to eclipsing objects through TTV plots (also known as "O-C" diagrams for Observed minus Calculated), that highlight differences between observed variations and calculated models [11, 12].

A few cases have used uTTVs to find evidence of unobserved, hidden planets in specific systems. Ballard et al. 2011 found evidence of an additional planet in Kepler-19 and found evidence of upper limits for its orbital period and mass of  $> 160$  days and  $> 6 M_{\text{Jup}}$  [13]. Precise parameters could not be determined due to degeneracies, however these limits confirm the planetary status of the object [13]. *Kepler* TTV signals are typically dominated by planet-planet interactions near mean motion resonances, which produces sinusoidal TTVs. A mean motion resonance refers to when two bodies have periods that are a simple integer ratio of each other leading to stronger interactions. In most cases, only the amplitude, period, and phase of the TTV sinusoid are known, but the same sinusoidal signal can be produced by planets near a variety of resonances.

The technique of studying uTTVs was also used by Nesvorný et al. 2013 to find a non-transiting companion to KOI-142.01 [14]. They used transit duration variations to further constrain the values of this hidden planet which broke degeneracies and allowed them to identify a specific planet. Later, this planet was confirmed through the radial velocity method [14, 15].

In this work, we look at 46 *Kepler* multis where one planet experiences well-detected TTVs not ascribed to a particular perturbing planet by [16]. We use these signals to predict hidden planets in the widest scale application of this technique to date.

There are also many ( $\sim 150$ ) systems where a single KOI experiences TTVs which, by definition, must be due to a hidden planet. We do not explore these systems here for multiple reasons. First, while most of these KOIs are likely to be due to true exoplanets, some could be due to

"false positives" like misinterpreting an eclipsing binary star. False positives are far less likely in multis [17]. Second, there are fewer constraints on the possible positions of hidden planets in singles than there are in multis. Finally, single KOIs are not as information-rich as multis and we chose to focus on multis as the most valuable systems for our additional study.

# Chapter 2

## Methods

To search for the cause of the TTVs in these systems, we primarily used the PhotoDynamical Multi-planet Model (PhoDyMM) developed by [18] for our analyses. PhoDyMM combines aspects of photometric and dynamical models to produce stellar lightcurves. It uses Differential Evolution Markov Chain Monte Carlo (DEMCMC) method to adjust the orbital and physical parameters of the planets to match the observed lightcurves. At each step, PhoDyMM evaluates  $\chi^2$ , a measure of goodness of fit evaluated using standard Gaussian statistics for independent data with the reported uncertainties (common for Kepler lightcurves that have been detrended like ours). Since each lightcurve has a different number of observations (due to how *Kepler* worked and the use of both "Long Cadence" and "Short Cadence" data), it was convenient to estimate the "reduced"  $\chi^2$ , which should be close to 1 for a good fit and for which smaller values indicate better fits. It is important to note here that PhoDyMM is fitting to the lightcurve directly and not to the TTV data. Although a good fit to the lightcurve should match the TTVs, they are not directly related and we saw some cases where better fits to the overall data did not have great fits to the TTV data.

We used PhoDyMM to look at the parameters for each planetary system we analyzed. We adjusted the values for planetary mass, radius, and orbital period. PhoDyMM created TTV plots of the modeled system's transits versus the data as well as plots of the TTV signal of each planet.

Figure 2.1 show samples of the plots produced by PhoDyMM. Subfigure (a) shows the modeled TTVs for the perturbed planet in KOI-759, where KOI stands for "Kepler Object of Interest". The red points with uncertainties represent the TTV data for this planet while the blue dots are the produced model. For this system, it is clear the best known planet model did not produce a good fit to the data because most of the data are not even visible (this plot is zoomed in to the model). Subfigure (b) shows the best hidden planet model for the same system. The blue dots here are the model with a hidden planet and it can be seen that it matches the red data points much more closely than the best known planet model. Subfigure (c) (middle column) shows the modeled lightcurves for this system using the best known planet parameters and subfigure (d) (right column) are the lightcurves for the best hidden planet model. These plots show the transits of the two known planets with the black dots representing the data and the red points representing the model. Again, it can be seen that this is not a good fit as the red transits do not match what is observed while the best hidden planet model matches the data very well.

This project was, at first, the class research project for the Fall 2019 Physics 227 class at Brigham Young University (BYU), taught and organized by Dr. Darin Ragozzine. After producing several of these key plots, each student in the class was given one system to do the preliminary analysis on and then all of the data was gathered for more in-depth work. We intend to publish this work with all the students as co-authors. After the work done by the individual students, we did longer calculations using BYU's supercomputer ("Mary Lou").

## 2.1 Known Planet Models

We started our analysis by modeling only the known planets in the systems. Each system has at least two confirmed planets, one of which is experiencing TTVs not obviously caused by any of the other planets. We first made adjustments to the known planets' masses to try and match the observed



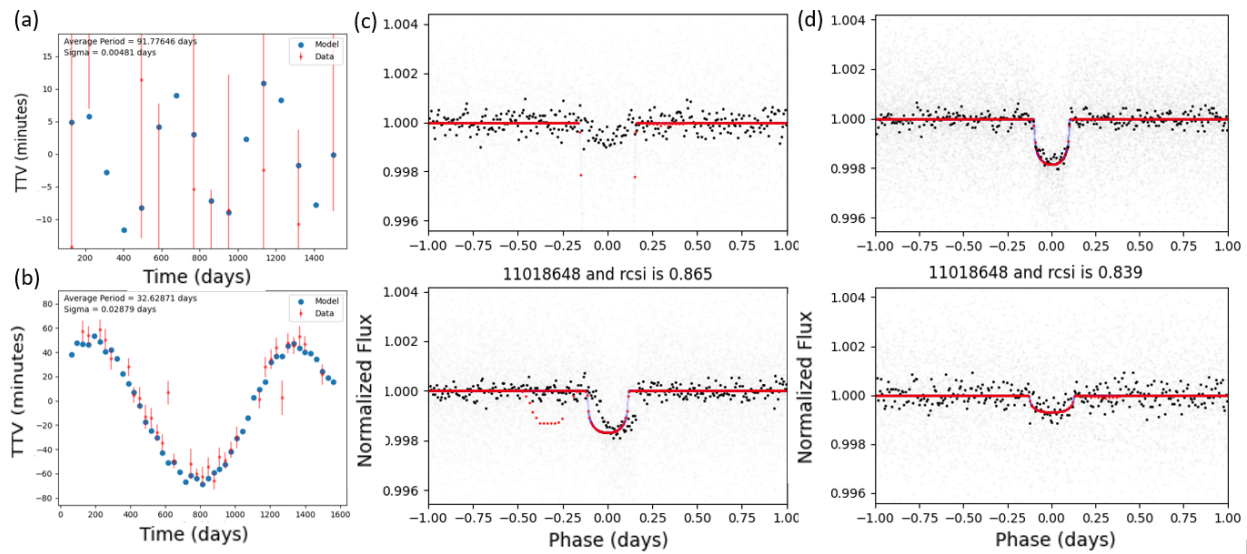


**Figure 2.1** Sample plots for system KOI-759. Subfigure (a) shows the best known planet TTV model. The red points with error bars are the data points while the blue dots are the model. Subfigure (b) is the best hidden planet TTV model. Again, the red points are the data while the blue are the model. Subfigure (c), the middle column, are the lightcurves for the best known planet model. The dip in stellar brightness for the transit of each planet is modeled. Subfigure (d), the right column, are the lightcurves for the best hidden planet model. For both subfigures (c) and (d) the black dots are the data points and the red dots are the model lightcurve. It can be seen the hidden planet model (a) matches the TTVs much better than the known planet model (b), as do the hidden planet lightcurves, (d) versus (c).

TTV amplitude as these are nearly linearly related. After matching the amplitude, we would attempt to match the TTV signal period. The relationship between TTV period and perturbing planet orbital period is non-linear, but specific (see below). Since Kepler data constrains the periods tightly, for many systems it was not possible to match the TTV period using the known planets. Sometimes the eccentricity and argument of periapse (eccentricity orientation angle) were changed to better match the observed TTV phase.

The models produced by PhoDyMM included a statistical analysis of how well it fit the lightcurve data. With each change of parameters, we made a new model and analyzed how it fit the data. We first focused on manually changing the parameters to make large changes in the output. Once we had a good overall fit, we started allowing PhoDyMM to perform longer DEMCMC runs. Our final analyses on the supercomputer involved 100 walkers going 10,001 steps. We did not ensure each system had run to convergence as that is beyond the scope of this paper.

## 2.2 Hidden Planet Models

We performed the same analysis for each system with an additional hidden planet as we did with the known planets. Using PhoDyMM, we changed the parameters of the added hidden planet to try and create a good fit to the data.

We know TTVs are caused by strong planet-planet interactions and so to predict likely hidden planets, we projected several possibilities in strong, small-integer orbital period resonances with the TTV-experiencing planet. We tested the following [p,q] resonance values: [4,3], [3,2], [2,1], [1,2], [2,3], [3,4]. For each of these projected hidden planets, the period  $P_h$ , mass  $M_h$ , semi-major axis  $a_h$ , and mutual Hill radius  $R_H$  relative to all known planets in the system were found.

PhoDyMM requires a good initial guess for the properties of the hidden planet. Following analytical studies of how TTVs are most commonly produced in *Kepler* data [19], we reversed these

to determine the key properties of the hidden planet. For example, the hidden planet's period is determined using:

$$P_h = \left| \frac{q}{\frac{p}{P_u} \pm \frac{1}{P_{\text{TTV}}}} \right| \quad (2.1)$$

where  $P$  refers to period and we use the subscript "u" to refer to the planet experiencing uTTVs and "h" to refer to the hidden planet.  $P_{\text{TTV}}$  is the observed period of TTVs, taken either from [16] or by inspection of the TTV data. In some cases, the true TTV period was longer than the four-year duration of the Kepler data so our estimates of  $P_{\text{TTV}}$  were not always accurate.

Note that  $\frac{p}{P_b} + \frac{1}{P_{\text{TTV}}}$  is used for resonances where  $p > q$  (the uTTV planet has a longer period than the hidden planet). The form  $\frac{p}{P_b} - \frac{1}{P_{\text{TTV}}}$  is used when  $p < q$  (the uTTV planet has a shorter period than the hidden planet).

The mass of the hidden planet  $M_h$  is then approximated by the following relationship:

$$M_h \simeq 2\pi \left( \frac{A_{\text{TTV}}}{P_{\text{TTV}}} \right) \left( \frac{p}{q} \right) M_s \quad (2.2)$$

where  $A_{\text{TTV}}$  is the amplitude of the TTV signal,  $P_{\text{TTV}}$  is the TTV period, and  $M_s$  is the mass of the star for the system. Note that the mass of the uTTV-experiencing planet  $M_u$  is not a strong determinant in the amplitude of the TTVs.

Finally, the semi-major axis is found for each of the six projected hidden planets. All of these values are used to make a preliminary measurement of the stability of the proposed planet. This is done by determining the number of mutual Hill radii between the hidden planet and all other planets in the system. The mutual Hill radius  $R_H$  is found by the equation:

$$R_H = \left( \frac{M_h + M_p}{3M_s} \right)^{1/3} \left( \frac{a_h + a_p}{2} \right) \quad (2.3)$$

where the subscript "p" refers to a known planet in the system. The  $M$  variables are the mass of the hidden planet  $M_h$ , known planet  $M_p$  and star  $M_s$ , and  $a$  is the semi-major axis of the hidden  $a_h$

and known  $a_p$  respectively.

The distance between planetary orbits is then determined by the difference between semi-major axes in units of the calculated  $R_H$  value. This distance in mutual Hill radii ( $\Delta R_H$ ) is a good heuristic for long-term orbital stability (e.g., [20]), with  $\Delta R_H < 8$  being unlikely for typical exoplanetary systems. For each of the hidden planets associated with the six [p,q] resonances considered, we find the smallest value of  $\Delta R_H$  implied. When  $\Delta R_H < 8$ , the hidden planet is considered too close to one of the other planets and the orbit is determined to be unstable. Of the remaining possibilities, we selected the planet in the strongest resonance (smallest  $p$ ).

Figure 2.2 shows an example of the projected hidden planets for system KOI-1601. This system has two known planets. Four of the projected hidden planets were in unstable orbits due to their proximity to the known planets in the system (specifically the uTTV planet) and were therefore eliminated as possibilities. Of the two remaining options, the [1,2] orbit is the stronger resonance and therefore the hidden planet with an orbit of 149 days (the orange line in Figure 2.2) was added to the system.

There is a high level of degeneracy in our prediction of hidden planet models. These degeneracies are because there are many possibilities of what hidden planet could be causing the TTVs observed in the system. There are far more unknowns about these planets than simple equations to try and solve them. For this reason the parameters we put forth for the hidden planets are preliminary values only. Other parameters for the hidden planet could cause the same resulting TTVs, for example a more massive planet that is farther from the uTTV planet. We do not attempt to break the degeneracies for each system as this would require a far more extensive analysis than the scope of this paper.

The other planetary properties were assumed to start at typical values: eccentricity of 0, inclination of 90, and orbital orientation angles of 0. Except for eccentricity, these properties are known to not be important for affecting TTVs. Although it is possible that these hidden planets are transiting

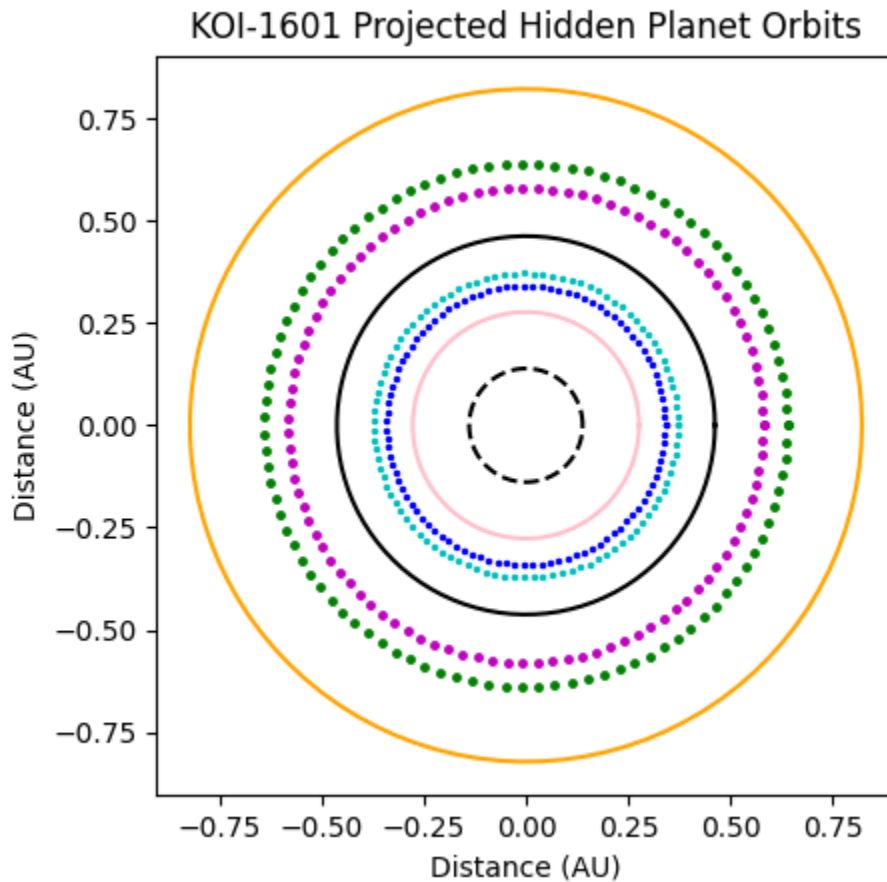


**Figure 2.2** Projected hidden planet orbits for KOI-1601. The black lines are the known planets in system KOI-1601. The dashed line is the non-TTV planet with a period of 10 days. The solid black line is the TTV-experiencing planet with a period of 65 days. The colored lines represent each of the projected resonance orbits for a hidden planet in the following order: pink - [2,1], blue - [3,2], cyan - [4,3], magenta - [3,4], green - [2,3], and orange - [1,2]. The dotted orbits are unstable because they are too close to the known planets in the system (black solid and dashed lines). The orange line is the strongest stable resonance for this system.

in a detectable way that was missed by *Kepler*, as our goal was to explain the uTTVs, we did not allow the transits of the hidden planet to explain the lightcurve by setting and fixing the radius of the planet to 0.

It is worthwhile to note that not all TTVs, including those under investigation here, are well explained by the sinusoidal near-resonant model we have chosen to determine the properties of hidden planets. TTVs are sometimes caused by higher-order resonances, non-resonant interactions, and other phenomena that we do not study here, adding additional models that could be degenerate with those we proposed. Some of our poorer fits may be attributed to the neglect of these possibilities.

With an initial guess for all the parameters of the hidden planet, it was added to the system. After adjusting the inputs to PhoDyMM, we then performed the same analysis as we did with the known planets: using PhoDyMM to find the best fit, but without a guarantee of convergence. Many parameters were adjusted by hand, especially in the early stages of the analysis.

# Chapter 3

## Results and Discussion

### 3.1 Results

Our hidden planet models produced remarkably good fits for the majority of the systems analyzed. Only five systems had better fits with only the known planets. For most systems, matching the observed uTTV amplitude required changing the mass (and/or eccentricity) of the perturbing planet to physically impossible values (e.g., densities implying compositions much more dense than pure iron). Good models were produced for 39 systems with the addition of a hidden planet. The remaining 2 systems require a more complicated answer than our analysis provided. One of these systems, KOI-1781, has been solved by [21] and we will include their results in our discussion below. Tables 3.1 and 3.2 provide a summary of the best fit parameters of every system we found good fits for.

As a reminder, these systems and planets were chosen specifically because they may have needed a hidden planet to explain their TTVs. That nearly all systems would require a hidden planet was expected. Furthermore, our list included some cases where the TTVs might have been caused by a known planet, but it was not certain. Thus, it is also not surprising that some cases were better

explained by a hidden planet model.

### 3.1.1 Systems with Best Fit Using Known Planets

Of the 46 systems in this analysis, we were able to find good fits for five using only the known planets. These systems are: KOI-89, KOI-111, KOI-156, KOI-464, KOI-1573. Table 3.1 shows the parameters used in the systems' respective best fit models. We tested how the addition of a hidden planet affected each of these systems. For some, there was a slight improvement to the statistical fit but this is likely due to the addition of more data and not an actual improvement. As our goal was to identify plausible explanations and not to explore every potential model in depth, we did not do a detailed statistical model comparison to validate our choice of model. In nearly all cases, the result was unambiguous.

Figure 3.1 shows the best model using the known planets for KOI-156.03. There is a strong fit to the observed data for this planet. The addition of a hidden planet did not significantly change this system. This is a typical example of the results for each of these systems. The parameters to produce these models can be found in Table 3.1. A discussion of each system with a best fit from the known planets will be included in A.1 along with one selected best fit figure in B.1.

Though these systems do not indicate the presence of a hidden planet, they are still very interesting because they result in a measurement (sometimes for the first time in the published literature) for the mass of a transiting planet. Less than 100 transiting planets have measured masses. PhoDyMM, which accounts for both the mass and radius of the known planets, is therefore able to constrain exoplanetary densities, of interest in understanding their composition. These densities are an important scientific contribution.



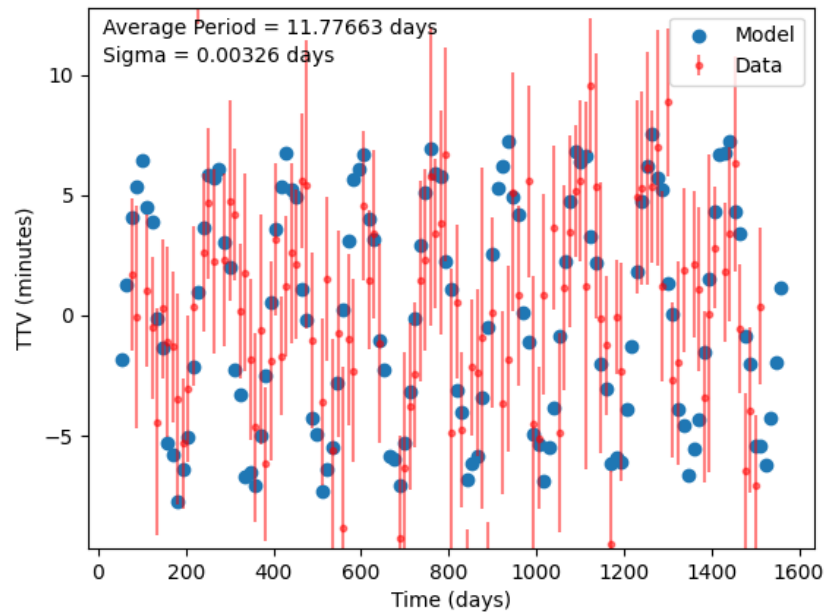


**Figure 3.1** The best known planet model for KOI-156. The red points are data with error bars. The blue dots are the model. It can be seen the model matches the data well in amplitude, period, and phase.

KOI	Num. Planets	Per (d)	Mass ( $M_{\text{Jup}}$ )	Rad ( $R_{\text{Jup}}$ )	uTTV Per (d)	uTTV Amp (min)
89	89.01	84.68	0.113	0.019	...	...
	89.02	207.59	0.025	0.023	1873.9	30
111	111.01	11.42	0.023	0.020	...	...
	111.02	23.66	0.023	0.019	...	...
	111.03	51.75	0.094	0.022	2108	3.5
156	156.02	5.188	0.003	0.016	...	...
	156.01	8.041	0.010	0.021	...	...
	156.03	11.77	0.022	0.033	164.4	3.2
464	464.02	5.350	0.023	0.026	...	...
	464.01	58.36	0.176	0.068	482.5	4.1
1573	1573.02	7.136	0.152	0.012	...	...
	1573.01	24.81	0.061	0.037	1504.7	90

**Table 3.1** Best fit planet parameters for systems with satisfactory known planet models. System planets are listed in order of their orbital periods. uTTV periods and amplitudes are only reported for the planet we studied. For the other planet in the system, we put "..." in these columns to indicate there is not a related value. A Jupiter mass  $M_{\text{Jup}}$  is  $1.899 \times 10^{27}$  kg and a Jupiter radius  $R_{\text{Jup}}$  is  $6.991 \times 10^5$  km.

### 3.1.2 Systems with Best Fit Using Hidden Planet

For the majority of our systems, their model was greatly improved by the addition of a hidden planet. Figure 3.2 shows an example of this for KOI-759. The known model could barely produce a recognizable TTV signal while the hidden model matches the data very well. Figure 3.2 is an example of a highly accurate fit. The planetary parameters for each system are summarized in Table 3.2. A description of the results for each system will be included in A.2 along with two selected best fit figures in B.2.

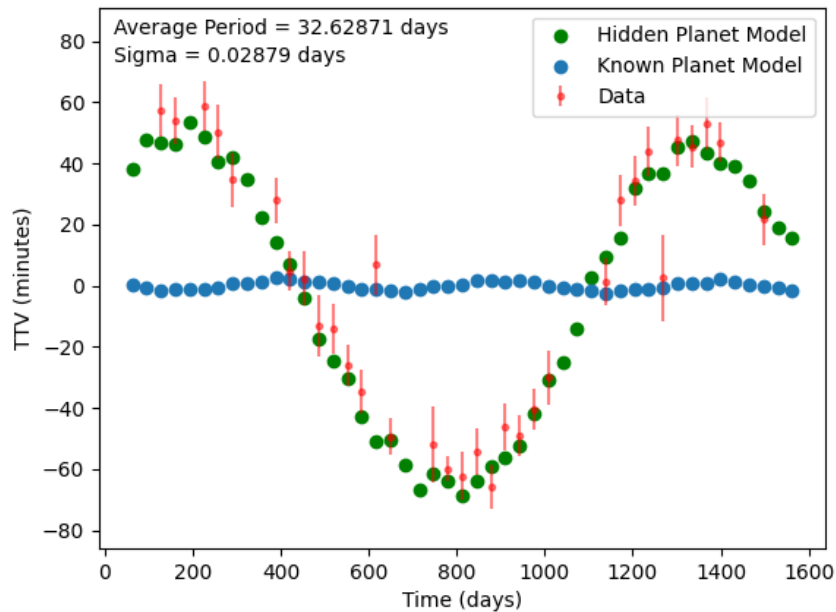


**Figure 3.2** The combined known and hidden best fit models for KOI-759. The red points are the data with uncertainty bars. The blue points represent the known planet model. The green points represent the hidden planet model. The hidden planet model clearly matches the data much better than the known planet model.

With these hidden planet parameters in place, many future analyses are enabled. The known planets can be studied in detail with PhoDyMM without concern that the inferred parameters are inaccurate due to a missing planet. When hidden planet masses indicate a radius that would be

detectable, the hidden planet must be non-transiting, with implications for the mutual inclination distribution of the planets. An obvious step for future researchers is to explore the degeneracies as it is possible that, in some cases, a unique model could be identified as clearly better, thus turning our potential hidden planets into a confirmed planet discovered through TTVs.

KOI	Num. Planets	Per (d)	Mass ( $M_{\text{Jup}}$ )	Rad ( $R_{\text{Jup}}$ )	uTTV Per (d)	uTTV Amp (min)
139	139.02	3.341	0.022	0.0080	...	...
	139.99	100.89	0.368	0.001	...	...
	139.01	224.77	0.209	0.057	986.1	50
289	289.01	26.62	0.031	0.020	489.4	5
	289.99	41.06	0.0016	0.001	...	...
	289.02	296.63	0.202	0.050	...	...
448	448.01	10.13	0.015	0.029	...	...
	448.02	43.57	0.0204	0.031	3000	70
	448.99	88.45	0.035	0.001	...	...
456	456.02	4.309	0.018	0.014	...	...
	456.01	13.69	0.057	0.032	877.5	20
	456.99	27.82	0.017	0.001	...	...
457	457.01	4.920	0.0040	0.0259	...	...
	457.02	7.064	0.0205	0.0277	283.7	8.5
	457.99	10.72	0.026	0.0020	...	...
481	481.02	1.553	0.199	0.018	...	...
	481.01	7.650	1.005	0.029	...	...
	481.03	34.26	0.053	0.029	344.4	5
	481.99	54.02	0.0015	0.0004	...	...

KOI	Num. Planets	Per (d)	Mass ( $M_{\text{Jup}}$ )	Rad ( $R_{\text{Jup}}$ )	uTTV Per (d)	uTTV Amp (min)
564	564.03	6.216	0.0018	0.0109	...	...
	564.01	21.09	0.062	0.012	1919	400
	564.99	42.57	0.0080	0.012	...	...
	562.02	127.90	0.798	0.059	...	...
598	598.01	8.306	0.155	0.024	537.1	9
	598.99	12.54	0.0094	0.0003	...	...
	598.02	34.09	0.396	0.019	...	...
638	638.01	23.63	0.0004	0.028	836.3	100
	638.99	36.09	0.0003	0.0032	...	...
	638.02	67.09	0.016	0.003	...	...
701	701.02	5.714	0.012	0.018	...	...
	701.05	12.44	0.0031	0.0094	...	...
	701.01	18.16	0.018	0.034	...	...
	701.99	74.65	0.0260	0.001	...	...
	701.03	122.38	0.017	0.024	439	10
	701.04	267.29	0.012	0.020	...	...
720	720.04	2.795	0.005	0.015	...	...
	720.01	5.690	0.031	0.034	...	...
	720.02	10.04	0.007	0.035	...	...
	720.04	18.36	0.046	0.034	674	4
	720.99	37.76	0.041	0.000	...	...
734	734.01	24.54	0.815	0.030	...	...
	734.02	70.27	0.196	0.026	425.1	70

KOI	Num. Planets	Per (d)	Mass ( $M_{\text{Jup}}$ )	Rad ( $R_{\text{Jup}}$ )	uTTV Per (d)	uTTV Amp (min)
	734.99	168.39	0.286	0.001	...	...
757	757.03	6.252	0.050	0.029	...	...
	757.01	16.06	0.0011	0.066	...	...
	757.02	41.19	0.0063	0.043	499.8	2
	757.99	64.45	0.0018	0.0092	...	...
759	759.99	16.09	0.012	0.0069	...	...
	759.01	32.62	0.152	0.038	1194	55
	759.02	91.79	0.151	0.024	...	...
872	872.02	6.763	0.012	0.011	...	...
	872.01	33.62	0.531	0.083	189.7	50
	872.99	81.74	0.907	0.001	...	...
884	884.03	3.335	0.011	0.018	...	...
	884.01	9.439	0.137	0.049	...	...
	884.02	20.47	0.014	0.0055	817.8	190
	884.99	42.007	0.150	0.012	...	...
1108	1108.02	1.475	0.123	0.011	...	...
	1108.03	4.152	0.263	0.014	...	...
	1108.01	18.92	0.707	0.025	568.8	8
	1108.99	39.15	0.098	0.001	...	...
1261	1261.02	15.19	0.0077	0.020	...	...
	1261.01	133.46	0.970	0.066	1690	7.5
	1261.99	289.80	0.0014	0.0021	...	...
1307	1307.02	20.34	0.019	0.027	...	...

KOI	Num. Planets	Per (d)	Mass ( $M_{\text{Jup}}$ )	Rad ( $R_{\text{Jup}}$ )	uTTV Per (d)	uTTV Amp (min)
	1307.01	44.84	0.0034	0.0296	789.1	15
	1307.99	95.10	0.0029	0.0030	...	...
1366	1366.01	19.25	0.0095	0.028	303.4	10
	H	29.82	0.00018	0.00059	...	...
	1366.02	54.15	0.212	0.034	...	...
1581	1581.01	29.54	0.025	0.026	964.6	95
	1581.99	60.95	0.039	0.0031	...	...
	1581.02	144.55	0.078	0.027	...	...
1601	1601.01	10.35	0.014	0.016	...	...
	1601.02	62.92	0.028	0.018	400	27
	1601.99	149.33	0.368	0.001	...	...
1613	1613.01	15.86	0.0010	0.0081	310.1	15
	1613.03	20.60	0.0078	0.0060	...	...
	1613.99	33.44	0.088	0.0060	...	...
	1613.02	94.09	0.0094	0.0072	...	...
1751	1751.01	8.689	0.039	0.031	...	...
	1751.02	21.00	0.039	0.030	5000	5
	1751.99	31.51	0.0020	0.001	...	...
1884	1884.02	4.790	...	0.163	...	...
	1884.01	23.09	0.057	0.020	1416.1	350
	1884.99	47.001	1.548	0.038	...	...
2061	2061.02	1.090	2.093	0.011	...	...
	2061.01	14.09	0.993	0.028	1056.1	160

KOI	Num. Planets	Per (d)	Mass ( $M_{\text{Jup}}$ )	Rad ( $R_{\text{Jup}}$ )	uTTV Per (d)	uTTV Amp (min)
	2061.99	28.553	0.041	0.001	...	...
2073	2073.02	6.474	0.043	0.021	...	...
	2073.03	16.85	0.461	0.029	...	...
	2073.01	49.50	0.137	0.028	739.2	20
	2073.99	67.22	0.025	0.001	...	...
2150	2150.99	9.195	0.0045	0.013	...	...
	2150.01	18.50	0.201	0.023	1500	20
	2150.02	44.70	0.018	0.017	...	...
2199	2199.02	3.052	0.102	0.014	...	...
	2199.01	9.033	0.379	0.027	33.6	20
	2199.99	18.15	0.014	0.0024	...	...
2466	2466.01	3.171	0.0018	0.0130	...	...
	2466.02	13.29	0.0028	0.0129	647.4	20
	2466.99	27.15	0.093	0.001	...	...
2650	2650.02	7.053	0.157	0.017	...	...
	2650.01	34.99	0.253	0.0089	234.8	50
	2650.99	82.23	...	0.011	...	...
2714	2714.01	14.38	0.146	0.012	...	...
	2714.02	47.32	0.018	0.017	724.5	20
	2714.99	101.26	0.103	0.0032	...	...
	2714.03	184.29	0.028	0.018	...	...
3057	3057.02	10.61	0.124	0.0204	...	...
	3057.01	29.73	0.0054	0.0281	792.7	30



KOI	Num. Planets	Per (d)	Mass ( $M_{\text{Jup}}$ )	Rad ( $R_{\text{Jup}}$ )	uTTV Per (d)	uTTV Amp (min)
	3057.99	61.77	0.290	0.281	...	...
3068	3068.99	1.94	0.051	0.0023	...	...
	3068.01	3.916	0.121	0.012	349.1	20
	3068.02	6.651	0.431	0.010	...	...
3184	3184.03	4.020	0.076	0.004	...	...
	3184.01	7.547	0.046	0.004	866.2	50
	3184.99	15.21	0.042	0.0001	...	...
3271	3271.02	7.418	0.137	0.013	...	...
	3271.01	19.55	0.011	0.023	710	40
	3271.99	40.20	0.012	0.0011	...	...
3319	3319.03	3.545	0.028	0.005	925.4	15
	3319.99	5.328	0.071	0.0002	...	...
	3319.02	8.239	0.025	0.013	...	...
	3319.01	19.59	0.015	0.016	...	...
3374	3374.01	9.508	0.0014	0.0086	731.1	7
	3374.99	14.35	0.0014	0.011	...	...
	3374.02	34.10	0.022	0.011	...	...

**Table 3.2** Planet parameters for systems with best model using a hidden planet. Planets designated as "KOI#.99" are the added hidden planet for the system. Each system is ordered by period. The uTTV period and amplitude are only reported for the planet we studied in this analysis. For the other planet in the system, we put "..." in these columns to indicate there is not related value. A Jupiter mass  $M_{\text{Jup}}$  is  $1.899 \times 10^{27}$  kg and a Jupiter radius  $R_{\text{Jup}}$  is  $6.991 \times 10^5$  km.

### 3.1.3 Systems with More Complicated Answers

Two of the systems we analyzed proved more complicated than the analysis we did. These two systems are KOI-1781 and KOI-3061. KOI-1781 has been solved previously in [21]. When picking systems for this project, we tried to find systems where only one planet showed uTTVs. KOI-3061 has two known planets, both with a significant TTV signal not caused by the other. This complicated our analysis and prevented our finding a satisfactory model. A description for each of these systems will be included in A.3 along with figures for best fits in B.3.

## 3.2 Conclusion

Our analysis was able to find a good model for most (all but two) of our 46 systems. This data provides a strong basis for further research in these systems to confirm the presence of any of the projected hidden planets. These models help to further constrain the parameters of all the planets in the system. They give us a better understanding of how these systems interact dynamically and give insight into the demographics of exoplanetary systems.

Future work for these systems could involve breaking some of the degeneracies behind the hidden planets. This would lead to determining more precisely the parameters of these planets and potentially detecting them through more direct methods. It is possible some of these planets are transiting but their signals have not previously been distinguished. There is much room for discovering new planets through these projected models.

# Appendix A

## System Descriptions

### A.1 System Description for Known Planet Models

#### **KOI-89 // KIC 8056665**

KOI-89 has less data than most of the other systems making it more difficult to determine fit accuracy. Both models produced somewhat messy lightcurves for the system. The known planet model produced a better match in the TTV plot.

#### **KOI-111 // KIC 6678383**

Both our known and hidden planet models for this system produced relatively good fits. The TTV plot for the uTTV planet looks to be a better fit to the data, however. The hidden planet model seemed to match the shape of the TTVs well but had a flipped phase (peaked during troughs and vice versa).

#### **KOI-156 // KIC 10925104**

Both known and hidden models are good fits to the data. The known planet model is preferred for being simpler. It also matches the data better in some cases than the hidden planet model. See Figure B.1.

**KOI-464 // KIC 8890783**

Both known and hidden models produced good fits to the lightcurves for the system. The TTV plots for the uTTV planet were significantly better for the known planet system.

**KOI-1573 // KIC 5031857**

KOI-1573 was a more difficult system to work with. There was only a small amount of data to compare the model to making it harder to determine the fits accuracy. Both models have their weaknesses, but the known planet models better fits the TTVs.

## A.2 System Description for Hidden Planet Models

**KOI-139 // KIC 8559644**

This system is known to also have transit duration variations, where the time it takes for the planet to transit changes. These are also caused by interactions between planets. Our model did not specifically take this into account, though PhoDyMM is able to match such duration variations well when explored. The known planet model requires an impossibly massive perturbing planet to match the TTV amplitude. The hidden planet model matches the data much better. This system has a low number of data points making it more difficult to determine fit accuracy.

**KOI-289 // KIC 10386922**

The known planet model can roughly match some of the TTV parameters, but not particularly well. The hidden planet model is a much closer fit to the data. It also creates a better system lightcurve.

**KOI-448 // KIC 5640085**

The known planet model does not match the shape of the TTV curve at all. The Rowe data (what is shown in the plot) for this system is very different from the Holczer data which is acknowledged to be more accurate. The hidden planet model matches the Holczer data, though not the displayed

Rowe data.

**KOI-456 // KIC 7269974**

The known planet model does not create a distinct shape to the TTVs and cannot match the data. The hidden planet model matches quite well and maintains reasonable physical parameters. The lightcurve for the system also fits better with the hidden planet model.

**KOI-457 // KIC 7440748**

The TTV period from the known planet model is a little too short for the data. It would require changing the period of the perturbing planet too much to create the observed TTV period. The hidden planet model matches the TTV signal better. The overall transiting lightcurve fit is not significantly better with the hidden planet model.

**KOI-481 // KIC 11192998**

The known planet model requires an impossibly large mass to match the TTV amplitude. The TTV shape also does not match the data. The lightcurve for the system looks about the same with both models. The hidden planet model matches the TTV shape much better and maintains reasonable physical parameters. See Figure B.2.

**KOI-564 // KIC 6786037**

This system has a low number of available data points making it more difficult to determine fit accuracy. The known planet model produces a very different TTV shape to the data. The hidden planet model matches the amplitude and period much better though the phase is still different from the data.

**KOI-598 // KIC 10656823**

The known planet model does not match the period of the TTV data. It can mostly match the amplitude of the TTVs but the hidden planet model matches both period and amplitude better. This system has comparatively large error bars making determining fit accuracy more difficult.

**KOI-638 // KIC 5113822**

The known planet model cannot produce the observed TTV amplitude without vastly changing the transiting lightcurves of the system. The hidden planet model produces a better fit without changing the overall lightcurves.

**KOI-701 // KIC 9002278**

The known planet model requires an impossibly massive perturbing planet to match observed TTVs. This system has 5 known planets and we primarily looked at the closest planet to the uTTV planet. It is possible therefore that a more complicated combination of interactions from the known planets could produce the observed TTVs. The hidden planet model produces a good fit. This system only has a few data points to compare to making it more difficult to determine fit accuracy.

**KOI-720 // KIC 9963524**

The known planet model could not produce a recognizable TTV signal. The model ends up looking shapeless. The hidden model matches the amplitude and period of the TTVs though its shape is also slightly different from the data.

**KOI-734 // KIC 10272442**

The known planet model has too long a TTV period and requires an impossibly high mass to match the data's amplitude. The hidden planet model matches both TTV period and amplitude. It maintains reasonable physical parameters and produces a better system lightcurve.

**KOI-757 // KIC 10910878**

The known planet model requires an impossibly massive perturbing planet to match the TTV amplitude. The TTV period is also too small with this model. The hidden planet model matches the TTV data very well. The system lightcurve is also a very good fit. See Figure B.3.

**KOI-759 // KIC 11018648**

The known planet model requires an impossible massive perturbing planet to match the TTV amplitude. It also has far too short a TTV period. The hidden planet model matches the data extremely well. The lightcurve fits the data much better with the hidden planet model. See Figure

3.2 earlier in this paper.

**KOI-872 // KIC 7109675**

The known planet model requires an impossibly high mass to match the TTV amplitude. It also has too long a TTV period. The lightcurves for the system look better with the known planet model, however. The hidden planet model matches the data TTV very well. This system has a very short period which can make the TTV plot more difficult to read.

**KOI-884 // KIC 7434875**

The known planet model would need an impossibly massive perturbing planet to match the observed TTV amplitude. It also creates a shapeless TTV curve. For this system, the Rowe and Holczer data are fairly different. The hidden planet model matches the TTV from the Holczer data.

**KOI-1108 // KIC 3218908**

The known planet model cannot produce the observed TTV amplitude without significantly changing the depth of the transits in the system lightcurves. The TTV shape also does not fit the data. The hidden planet model produces a good TTV and lightcurve fit.

**KOI-1261 // KIC 8678594**

This system has fewer data points making it more difficult to determine the fit accuracy. The known planet model does not well match the shape of the TTVs and produces a lightcurve model that is not as good as the hidden planet model. The hidden planet model fits the shape and amplitude of the TTVs much better.

**KOI-1307 // KIC 10973814**

The known planet model would need an impossible massive perturbing planet to match the TTV amplitude. The TTV period and phase also do not match the data. The hidden planet matches the amplitude and period while maintaining physically reasonable parameters. It also produces a better system lightcurve.

**KOI-1366 // KIC 6932987**

Both models are decent matches to the data. The known planet model has a bit shorter of a TTV period. The hidden planet model matches very well. Both produce good fits to the system lightcurve.

**KOI-1581 // KIC 7939330**

The shape of the curve for this system is more complicated than most of the systems. The known planet model only matches part of the curve. It requires an impossibly high massive to match the TTV amplitude. The hidden planet model matches the whole TTV shape better and maintains reasonable physical parameters.

**KOI-1601 // KIC 5438757**

Both known and hidden models produced fairly good fits, however the hidden planet model more closely matched the TTVs. This fit is a little more tenuous and with more work it may prove that the known planets could produce the observed TTVs.

**KOI-1613 // KIC 6268648**

The known planet model created a TTV with too long a period for the data. It also did not produce a good lightcurve fit to the system. The hidden planet model matches the data TTV period and amplitude very well.

**KOI-1751 // KIC 9729691**

The known planet model would require an impossibly massive perturbing planet to match the TTV amplitude. It also does not well match the lightcurve for the system. The hidden planet matches the lightcurve better. It matches the Holczer data for the TTV which is more extensive than the shown Rowe data.

**KOI-1884 // KIC 4851530**

For this system, the Holczer and Rowe data does not match well. The known planet model produces a very odd TTV signal that does not match the data. The hidden planet model matches the data better.



**KOI-2061 // KIC 12061969**

The known planet model requires an impossibly massive perturbing planet to match the observed TTV amplitude. The hidden planet maintains reasonable parameters and better matches the shape of the TTV signal.

**KOI-2073 // KIC 8164257**

The known planet model will not match both amplitude and period. The two values are close enough that they start to affect each other and the known model cannot match both at once. The hidden planet model matches the amplitude and period, however.

**KOI-2150 // KIC 3229150**

The known planet model does not produce TTVs with a recognizable shape or periodicity. The hidden planet model matches the overall shape of the data but misses some of the inner structures.

**KOI-2199 // KIC 11705004**

The known planet model would require an impossibly massive planet in order to match the observed TTV amplitude. The shape of the TTVs also does not match the data with the known planet model. The hidden planet model fits the data much better and maintains physically reasonable parameters.

**KOI-2466 // KIC 8544992**

The data for this systems has fairly large error bars relative to the TTV amplitude. This makes it harder to determine the accuracy of the fit. The known planet model does not match the shape of the TTV data. The hidden planet model looks to be a much better fit.

**KOI-2650 // KIC 8890150**

The known planet model does not create a TTV with a distinct shape. The hidden planet model matches the shape well. The transits for this system are very shallow making it more difficult to determine how well the lightcurves fit.

**KOI-2714 // KIC 12206313**

The known planet model produces too short a TTV period to match the data. It also requires an impossibly high mass to match the amplitude. The hidden planet model matches the data much better and maintains reasonable physical parameters.

**KOI-3057 // KIC 3234843**

The known planet model cannot create the observed TTV amplitude with a reasonable mass. The phase and shape of the TTVs are also different from the data. The lightcurve for the system looks good with both fits. The hidden planet model fits the observed TTV signal very well. This system has a quite unique TTV shape.

**KOI-3068 // KIC 3230805**

The known planet requires an impossibly high mass to match the TTV amplitude. It matches the period quite well but the phase is off. The hidden planet model matches the data TTV quite well and maintains reasonable physical parameters.

**KOI-3184 // KIC 4735826**

This system has a false positive that is known as KOI-3184.02 which is the reason for the numbering for this system now being KOI-3184.01 and KOI-3184.03. Both models produce reasonable fits to the TTVs with acceptable physical parameters. The hidden planet model matches the data a little better and produces a better fit to the system overall.

**KOI-3271 // KIC 7285757**

The mass needed to match the observed TTV amplitude would produce an impossibly dense planet and thus eliminates the possibility of explaining the TTVs with the known planets. The shape of the TTV signal produced by the known planets also does not match the data. The hidden planet model matches the data much better.

**KOI-3319 // KIC 5965819**

This is a more difficult system as its TTVs have an unusual shape. The known planet model actually produces too high a TTV amplitude. This model also has too short a TTV period. The

hidden planet matches the amplitude of the data and has a much closer period though it is also a bit short with current values.

**KOI-3374 // KIC 6705026**

The known planet model produces a TTV that does not appear periodic. The hidden planet model matches the amplitude and period of the TTVs much better. The lightcurves for both models are a little messy but the overall fit is still within acceptable ranges.

### A.3 System Descriptions for Complicated Systems

**KOI-1781 // KIC 11551692**

Using model from [21]. None of our fits were able to fit the TTV data well. We found [21] after working on the system for some time and their fit works well so we did not pursue a more detailed explanation. See Figure B.4.

**KOI-3061 // KIC 4857058**

The known planet model requires an impossibly massive perturbing planet to match the TTV amplitude. The TTV shape is also very different from the data. The hidden planet model has some peculiarities to it but the match is much closer to the data. See Figure B.5.



# Appendix B

## Selected Best Fit Model Figures

### B.1 Best Fit for Known Models

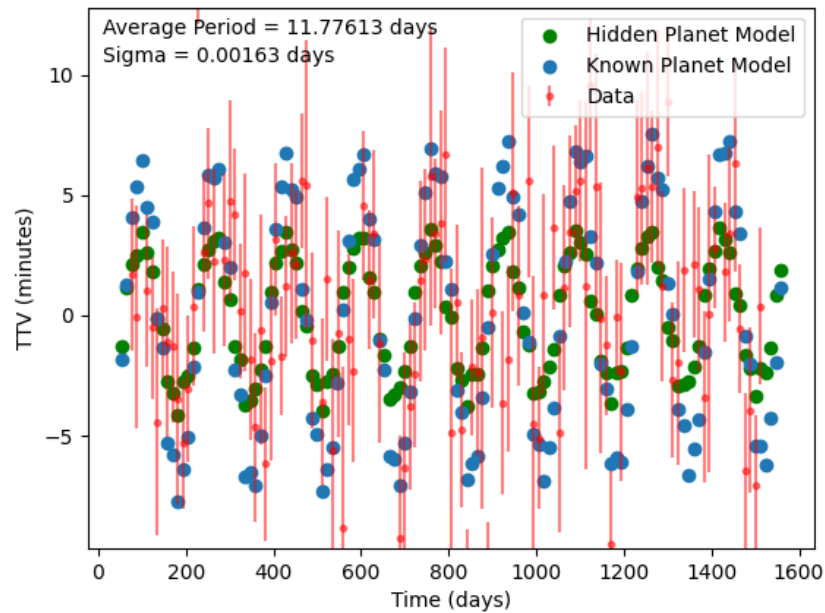


**Figure B.1** Combined best fits for KOI-156.03. The known model (blue) fits the data better than the hidden model (green).

## B.2 Best Fit for Hidden Models

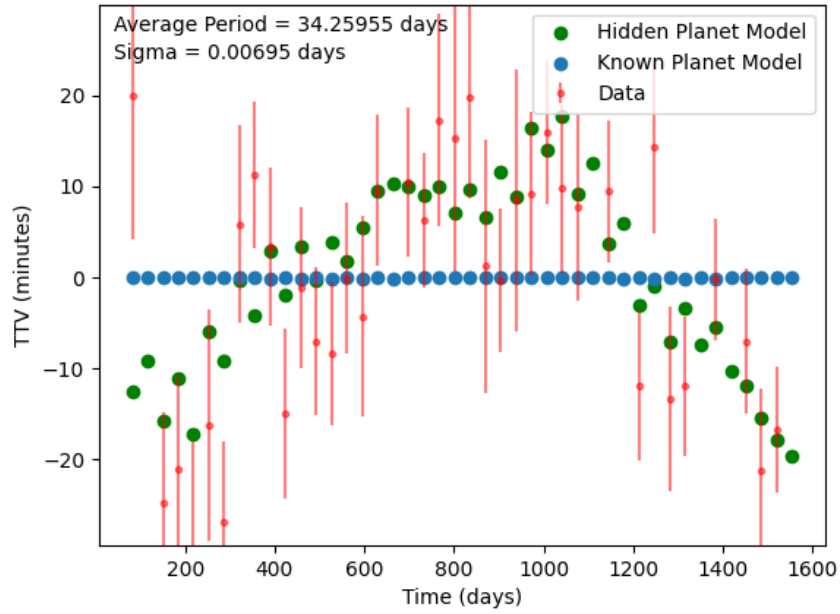


**Figure B.2** Combined best fits for KOI-481.03. The hidden model (green) fits the data much better than the known model (blue).

## B.3 Best Fit for Complicated Systems

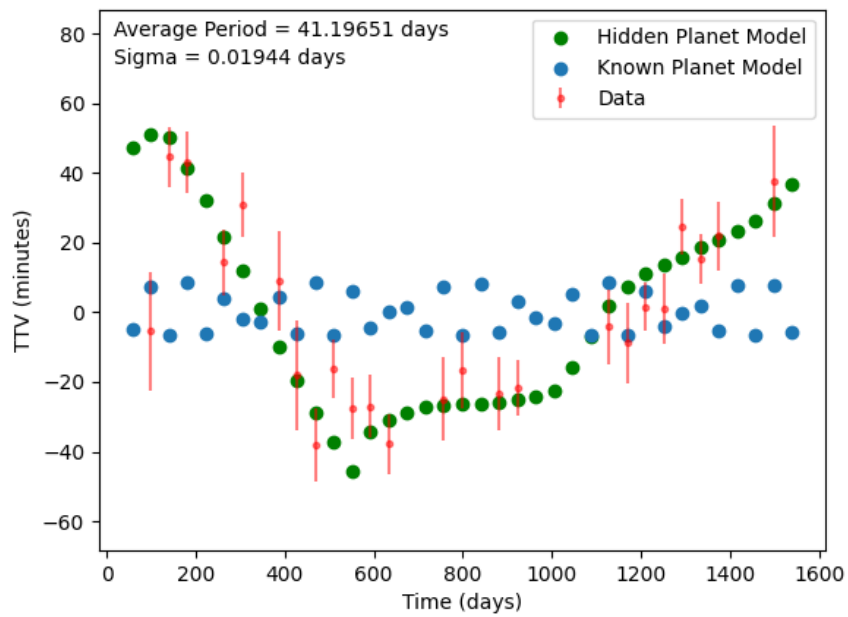


**Figure B.3** Combined best fits for KOI-757.02. The hidden model (green) fits the data much better than the known model (blue).

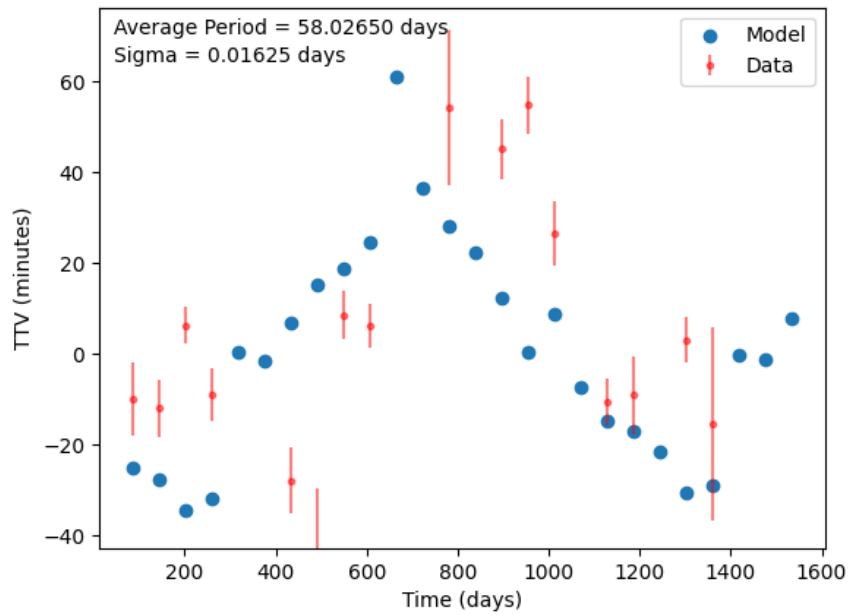


**Figure B.4** Best fit from [21] for KOI-1781.01. None of the fits produced by our models were able to recreate the data for this system.



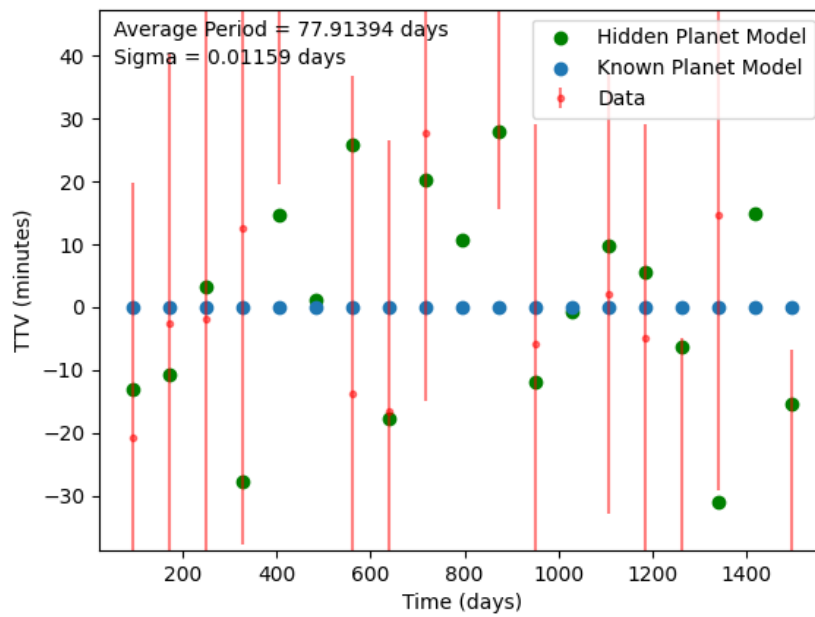


**Figure B.5** Combined best fits for KOI-3061.02. Neither model fits the data well. We were unable to find a reasonable fit for this system.



# List of Figures

1.1	Exoplanet Numbers by Discovery Method . . . . .	2
1.2	Exoplanets discovered by Kepler . . . . .	3
2.1	Sample output from PhoDyMM . . . . .	9
2.2	Possible hidden planets for KOI-1601 . . . . .	13
3.1	Example of best known planet model . . . . .	17
3.2	Example hidden best fit model . . . . .	19
B.1	KOI-156 . . . . .	37
B.2	KOI-481 . . . . .	38
B.3	KOI-757 . . . . .	39
B.4	KOI-1781 . . . . .	40
B.5	KOI-3061 . . . . .	41



# Bibliography

- [1] A. Wolszczan and D. A. Frail, “A planetary system around the millisecond pulsar PSR1257 + 12,” *Nature* **355**, 145–147 (1992).
- [2] B. Campbell, G. A. H. Walker, and S. Yang, “A Search for Substellar Companions to Solar-type Stars,” *Astrophysical Journal* **331**, 902 (1988).
- [3] W. D. Cochran, A. P. Hatzes, M. Endl, D. B. Paulson, G. A. H. Walker, B. Campbell, and S. Yang, “A Planetary Companion to the Binary Star Gamma Cephei,” In *AAS/Division for Planetary Sciences Meeting Abstracts #34*, AAS/Division for Planetary Sciences Meeting Abstracts **34**, 42.02 (2002).
- [4] NASA, “Exoplanet Plots - Detections per Year,” 2021.
- [5] E. Gaidos and A. W. Mann, “Objects in Kepler’s Mirror May be Larger Than They Appear: Bias and Selection Effects in Transiting Planet Surveys,” *The Astrophysical Journal* **762**, 41 (2013).
- [6] D. Ragozzine and M. J. Holman, “The Value of Systems with Multiple Transiting Planets,” arXiv e-prints p. arXiv:1006.3727 (2010).
- [7] N. M. Batalha, “Exploring exoplanet populations with NASA’s Kepler Mission,” *Proceedings of the National Academy of Science* **111**, 12647–12654 (2014).

- [8] R. Chen, “New Kepler Planet Candidates,” 2017.
- [9] C. J. Shallue and A. Vanderburg, “Identifying Exoplanets with Deep Learning: A Five-planet Resonant Chain around Kepler-80 and an Eighth Planet around Kepler-90,” *The Astronomical Journal* **155**, 94 (2018).
- [10] E. B. Ford *et al.*, “Transit Timing Observations from Kepler. I. Statistical Analysis of the First Four Months,” *The Astrophysical Journal Supplement* **197**, 2 (2011).
- [11] Z. Bozkurt and Ö. L. Değirmenci, “Triple systems showing apsidal motion,” *Monthly Notices of the Royal Astronomical Society* **379**, 370–378 (2007).
- [12] R. W. Slawson *et al.*, “Kepler Eclipsing Binary Stars. II. 2165 Eclipsing Binaries in the Second Data Release,” *The Astronomical Journal* **142**, 160 (2011).
- [13] S. Ballard *et al.*, “The Kepler-19 System: A Transiting  $2.2 R_{\oplus}$  Planet and a Second Planet Detected via Transit Timing Variations,” *Astrophysical Journal* **743**, 200 (2011).
- [14] D. Nesvorný, D. Kipping, D. Terrell, J. Hartman, G. Á. Bakos, and L. A. Buchhave, “KOI-142, The King of Transit Variations, is a Pair of Planets near the 2:1 Resonance,” *Astrophysical Journal* **777**, 3 (2013).
- [15] S. C. C. Barros *et al.*, “SOPHIE velocimetry of Kepler transit candidates. X. KOI-142 c: first radial velocity confirmation of a non-transiting exoplanet discovered by transit timing,” *Astronomy I& Astrophysics* **561**, L1 (2014).
- [16] M. Kane, D. Ragozzine, X. Flowers, T. Holczer, T. Mazeh, and H. M. Relles, “VizieR Online Data Catalog: Visual analysis and demographics of Kepler TTVs (Kane+, 2019),” *VizieR Online Data Catalog* p. J/AJ/157/171 (2019).

- 
- [17] J. J. Lissauer *et al.*, “Validation of Kepler’s Multiple Planet Candidates. II. Refined Statistical Framework and Descriptions of Systems of Special Interest,” *The Astrophysical Journal* **784**, 44 (2014).
- [18] D. Ragozzine, D. C. Fabrycky, and V. Sharma, “PhoDyMM: The PhotoDynamical Multiplanet Model for Exoplanet Density Inference,” (InPrep).
- [19] Y. Lithwick, J. Xie, and Y. Wu, “Extracting Planet Mass and Eccentricity from TTV Data,” *The Astrophysical Journal* **761**, 122 (2012).
- [20] A. Obertas, C. Van Laerhoven, and D. Tamayo, “The stability of tightly-packed, evenly-spaced systems of Earth-mass planets orbiting a Sun-like star,” *Icarus* **293**, 52–58 (2017).
- [21] L. Sun, P. Ioannidis, S. Gu, J. H. M. M. Schmitt, X. Wang, and M. B. N. Kouwenhoven, “Kepler-411: a four-planet system with an active host star,” *Astronomy and Astrophysics* **624**, A15 (2019).





# Index

degeneracy, 5, 12, 13, 26

exoplanets, 1, 2, 26

hidden planet model, 8, 10, 12, 15, 19, 25

figures, 38

systems, 28

Kepler, 4, 5

Kepler Space Telescope, iii, 2

known planet model, 8, 15–18

figures, 37

systems, 27

multis, iii, 4–6

PhoDyMM, 7, 8, 10

radial velocity, 5

stability, 13

mutual hill radius, 11

supercomputer, 8, 10

transit, 5

transiting, iii, 1, 5, 26

transits, 2, 4